

A Computational Model of the Electromagnetic Heating of Biological Tissue with Application to Hyperthermic Cancer Therapy

PETER M. VAN DEN BERG, A. T. DE HOOP, A. SEGAL, AND N. PRAAGMAN

Abstract—To investigate the potentialities of hyperthermia as a cancer therapy, computer simulations have been performed. This simulation consists of two successive steps. First, the heat generated in a distribution of biological tissue when irradiated by a source of electromagnetic radiation is computed. The mathematical tool for determining the distribution of generated heat is the domain-integral-equation technique. This technique enables us to determine in a body with arbitrary distribution of permittivity and conductivity the electromagnetic field due to prescribed sources. The integral equation is solved numerically by an iterative minimization of the integrated square error. From the computed distribution of generated heat, the temperature distribution follows by solving numerically the pertaining heat transfer problem. The relevant differential equation together with initial and boundary conditions is solved numerically using a finite-element technique in space and a finite-difference technique in time. Numerical results pertaining to the temperature distribution in a model of the human pelvis are presented.

I. INTRODUCTION

IN the investigation of the potentialities of hyperthermia techniques in cancer therapy [1], the computational modeling of the temperature distribution in an inhomogeneous distribution of tissue that is heated by electromagnetic radiation is an important tool. Through it, one can gain insight into the influence that different tissue parameters and organ's size, shape, and relative position have on the temperature distribution at hand, before actual experiments *in vivo* are carried out. Although the real problem is three-dimensional in nature, the handling of three-dimensional structures of realistic size and degree of complexity is beyond the reach of many of the present-day computer systems. In the present paper we have employed a two-dimensional approximation that applies to structures that in one direction (the axial direction) vary much less rapidly than in the plane transverse to it (the transverse plane). In regions of the human body where such an approximation roughly holds, the influence of the different organs and tissue distributions, as well as the positioning of the source of electromagnetic radiation, can be studied.

In the range of temperatures that are used in hyperthermia,

the change of the physical parameters such as permittivity, electrical conductivity, thermal conductivity, volume density of mass, and specific heat capacity with temperature is negligible. This implies that the electromagnetic field distribution problem can be handled separately from the heat transfer problem. With the electromagnetic field intensities involved, the electromagnetic problem is a linear one. In the heat transfer problem only the cooling due to blood circulation must be taken into account in a nonlinear way.

In the present paper, computer simulations are reported. First, the heat generated in a distribution of tissue irradiated by a source of electromagnetic radiation is computed. The mathematical tool for this is the domain-integral-equation technique. This technique enables us to determine in a body with arbitrary distribution of permittivity and conductivity the electromagnetic field due to prescribed sources. Iskander, Maini, Durney, and Bragg [2], Iskander and Durney [3], and Iskander, Turner, DuBow, and Kao [4] have performed a similar technique to calculate the electromagnetic field in a two-dimensional model of tissue. After discretization they replaced the integral equation by a linear system of algebraic equations. In the present paper the problem of excessive computer time and computer storage required for the direct numerical solution of the system of equations has been avoided: the integral equation is solved numerically by an iterative minimization of the integrated square error [5]. We show that even a subdivision of the two-dimensional cross section of the body into some three thousand equally sized squares can be handled efficiently. From the computed distribution of generated heat, the temperature distribution follows by solving numerically the pertaining heat transfer problem. The relevant partial differential equation is solved numerically using a standard finite-element technique in space and a finite-difference method in time. Finally, numerical results pertaining to the temperature distribution in the tissue of a representative human pelvis are presented. The values of the physical parameters of tissue that play a role in the electromagnetic part and in the heat transfer part of the problem are the input parameters of the developed computer programs. These values are chosen sufficiently realistic to be used in a computational model [6]; most of them can be found in the literature [7]–[16].

II. THE ELECTROMAGNETIC PROBLEM

In this section we investigate the electromagnetic part of the problem, i.e., the computation of the heat generated by the

Manuscript received October 18, 1982; revised May 3, 1983.

P. M. van den Berg and A. T. De Hoop are with the Laboratory of Electromagnetic Research, Department of Electrical Engineering, Delft University of Technology, 2600 GA Delft, The Netherlands.

A. Segal is with the Laboratory of Applied Analysis, Department of Mathematics and Information Sciences, Delft, University of Technology, Delft, The Netherlands.

N. Praagman is with Svasek B.V., The Netherlands, and the Dutch National Institute of Water Supply, The Netherlands.

TABLE I
PHYSICAL QUANTITIES AND CONSTITUTIVE PARAMETERS OCCURRING IN
THE ELECTROMAGNETIC PROBLEM

name	symbol	SI-unit
electric field intensity	\mathbf{E}	V/m
magnetic field intensity	\mathbf{H}	A/m
permittivity	$\epsilon = \epsilon_0 \epsilon_r$	F/m
permeability	$\mu = \mu_0 \mu_r$	H/m
electric conductivity	σ	S/m
volume density of generated heat power	\dot{w}_h	W/m ³
ϵ_0 (permittivity in vacuo) = 8.8544×10^{-12} F/m		
μ_0 (permeability in vacuo) = $4\pi \times 10^{-7}$ H/m		

electromagnetic field. The physical quantities and the constitutive parameters that play a role in this computation are listed in Table I. The irradiation of the tissues usually takes place through an electromagnetic field that varies sinusoidally in time and hence has a single frequency component. The complex representation of field quantities is used; they have the complex time factor $\exp(-i\omega t)$ (i = imaginary unit, ω = angular frequency, t = time) in common. This factor is omitted in the formulas. The location of a point in space is specified by its coordinates x_1 , x_2 , and x_3 with respect to a given, fixed, orthogonal Cartesian reference frame. It is assumed that in the domain of interest the configuration consisting of electromagnetic sources and irradiated tissue is independent of x_3 (two-dimensional approximation). We further assume that only the x_3 -component of the electric field is excited (E - polarization). Therefore, we have

$$E_1 = 0, E_2 = 0, E_3 = E. \quad (1)$$

In view of the organization of the computation, it is further advantageous to write the electric field intensity as the sum of the values of the incident field E^i and the scattered field E^s , i.e.,

$$E = E^i + E^s \quad (2)$$

where the incident field is the field that would be generated in the absence of the tissue, and the scattered field accounts for the reaction of the tissue on the incident field. Now, in our application (Fig. 1), the incident field emerges from a cooled ridged waveguide applicator. Experiments have shown that the aperture field is practically constant over its cross section and falls off rapidly near the boundaries, where it reduces to zero. Therefore, we approximate the electric and magnetic field by a constant value, the latter being proportional to the normal derivative of the electric field (Huygens' source aperture radiation). Neglecting the field on the outer boundary of the applicator outside the radiating aperture, the incident field follows from

$$E^i(\mathbf{x}) = \int_{\text{aperture}} [\partial'_\nu G(\mathbf{x} - \mathbf{x}') E^a(\mathbf{x}') - G(\mathbf{x} - \mathbf{x}') \partial'_\nu E^a(\mathbf{x}')] ds(\mathbf{x}') \quad (3)$$

where $\mathbf{x} = (x_1, x_2)$ is the point of observation in the cross section, $\mathbf{x}' = (x'_1, x'_2)$ is a point of the aperture, ∂'_ν is the de-

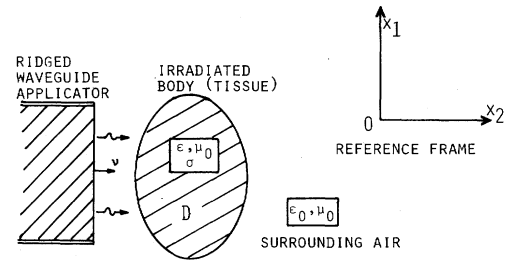


Fig. 1. Schematic cross section of the configuration.

rivative with respect to \mathbf{x}' in the direction of the unit normal ν to the aperture plane pointing toward the half space into which radiation takes place, E^a is the aperture field, and G is the two-dimensional free-space Green's function, given by

$$G(\mathbf{x} - \mathbf{x}') = \frac{i}{4} H_0^{(1)}(k_0 |\mathbf{x} - \mathbf{x}'|) \quad (4)$$

where $H_0^{(1)}$ denotes the Hankel function of the first kind and order zero, and $k_0 = \omega(\epsilon_0 \mu_0)^{1/2}$ denotes the wavenumber of the free space (air) surrounding the object. Further $|\mathbf{x} - \mathbf{x}'|$ denotes the geometrical distance from a point \mathbf{x}' of the aperture to the point of observation \mathbf{x} . Through an application of Helmholtz's integral formula [17] to the half-space into which radiation takes place, it can be shown that upon neglecting the field in the complement of the radiating aperture, (3) can be replaced by

$$E^i(\mathbf{x}) = 2 \int_{\text{aperture}} \partial'_\nu G(\mathbf{x} - \mathbf{x}') E^a(\mathbf{x}') ds(\mathbf{x}') \quad (5)$$

which is valid in any point of the half-space in front of the radiator. Once the aperture field has been prescribed, the incident field follows from (5).

In view of the high contrast in electromagnetic properties between the tissues to be irradiated and the surrounding free space (air), our computational scheme aims at the direct calculation of the total electric field in the interior of the irradiated object. Because of this and since the object itself has already a detailed structure, the domain-integral-equation is taken as the point of departure in the computations. The domain-integral-equation formulation takes into account that the irradiated object is present in free space, and that it manifests itself through the presence of secondary sources of contrast currents that in their turn are related to the contrast in electromagnetic properties. For two-dimensional E -polarized fields and for objects (tissue) showing contrast in electric properties (permittivity and conductivity) only, we have [18]

$$E(\mathbf{x}) = E^i(\mathbf{x}) + \int_D G(\mathbf{x} - \mathbf{x}') C(\mathbf{x}') dA(\mathbf{x}'), \quad \mathbf{x} \in D \quad (6)$$

in which D denotes the domain occupied by the object (tissue), and where

$$C(\mathbf{x}) = k_0^2 \chi(\mathbf{x}) E(\mathbf{x}) \quad (7)$$

denotes the contrast source density, with the electric contrast function χ given by

$$\chi(\mathbf{x}) = \epsilon/\epsilon_0 - 1 - \sigma/i\omega\epsilon_0. \quad (8)$$

TABLE II
THE LEAST-SQUARE ITERATIVE SOLUTIONS (STEEPEST-DESCENT METHOD)
OF THE INTEGRAL EQUATION (ASTERISK DENOTES COMPLEX CONJUGATE)

starting value	$E^{(0)}(\mathbf{x}) = E^i(\mathbf{x})$
	$c^{(0)}(\mathbf{x}) = k_0^2 \chi(\mathbf{x}) E^{(0)}(\mathbf{x})$
<hr/>	
$F^{(0)}(\mathbf{x}) = \int_D G(\mathbf{x}-\mathbf{x}') c^{(0)}(\mathbf{x}') dA(\mathbf{x}')$	
$ERR^{(0)} = \int_D F^{(0)}(\mathbf{x}) ^2 dA(\mathbf{x})$	
$n \geq 0$	
$e^{(n)}(\mathbf{x}) = F^{(n)}(\mathbf{x}) - k_0^2 \chi^*(\mathbf{x}) \int_D G^*(\mathbf{x}-\mathbf{x}') F^{(n)}(\mathbf{x}') dA(\mathbf{x}')$	
$c^{(n)}(\mathbf{x}) = k_0^2 \chi(\mathbf{x}) e^{(n)}(\mathbf{x})$	
$a^{(n)} = \int_D e^{(n)}(\mathbf{x}) ^2 dA(\mathbf{x})$	
$f^{(n)}(\mathbf{x}) = e^{(n)}(\mathbf{x}) - \int_D G(\mathbf{x}-\mathbf{x}') c^{(n)}(\mathbf{x}') dA(\mathbf{x}')$	
$b^{(n)} = \int_D f^{(n)}(\mathbf{x}) ^2 dA(\mathbf{x})$	
$n^{(n)} = a^{(n)}/b^{(n)}$, $E^{(n+1)}(\mathbf{x}) = E^{(n)}(\mathbf{x}) + n^{(n)} e^{(n)}(\mathbf{x})$	
$F^{(n+1)}(\mathbf{x}) = F^{(n)}(\mathbf{x}) - n^{(n)} f^{(n)}(\mathbf{x})$	
$ERR^{(n+1)} = ERR^{(n)} - n^{(n)} a^{(n)}$	
$n \approx n+1$	

In the frequencies range (27 MHz) and for configurations under present investigation the scattered field outside the human body turns out to have an almost constant value in amplitude and phase at the position where the radiating aperture is present. The reaction of this scattered field on the assumed (constant) aperture field can, therefore, be taken into account by multiplying the latter by a constant which depends on the irradiated body. In view of the applied normalization of generated heat, only the relative spatial distribution of the aperture field plays a role and hence absolute magnitudes are not computed. (In practice, the absolute value in the actual configuration is adjusted.)

The integral equation (6) will be solved numerically, using an iterative scheme of the type

$$E^{(n+1)}(\mathbf{x}) = E^{(n)}(\mathbf{x}) + \eta^{(n)} e^{(n)}(\mathbf{x}),$$

$$\mathbf{x} \in D, n = 0, 1, 2, \dots$$

The integrated square error after the n th iteration becomes

$$ERR^{(n)} = \int_D |F^{(n)}(\mathbf{x})|^2 dA(\mathbf{x}) \quad (10)$$

in which

$$F^{(n)}(\mathbf{x}) = E^i(\mathbf{x}) - E^{(n)}(\mathbf{x}) + \int_D G(\mathbf{x} - \mathbf{x}') C^{(n)}(\mathbf{x}') dA(\mathbf{x}') \quad (11)$$

while

$$C^{(n)}(\mathbf{x}) = k_0^2 \chi(\mathbf{x}) E^{(n)}(\mathbf{x}). \quad (12)$$

A convergent iterative procedure ($ERR^{(n+1)} < ERR^{(n)}$) is arrived at by minimizing (10) as a function of $\eta^{(n)}$ and choosing $e^{(n)}$ in accordance with steepest descent at $\eta^{(n)} = 0$. The structure of this least-square iterative technique is shown in Table II; more details can be found elsewhere [5]. As a starting value we have taken $E^{(0)}(\mathbf{x}) = E^i(\mathbf{x}), \mathbf{x} \in D$.

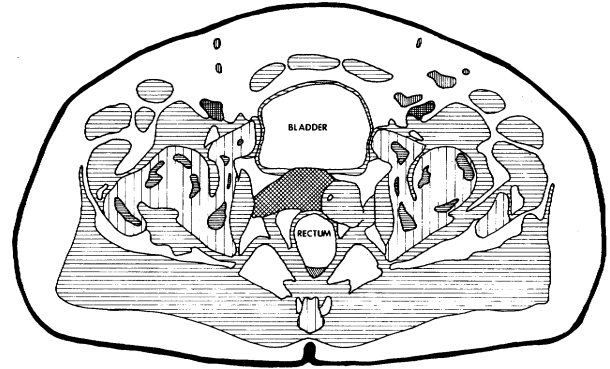


Fig. 2. Model of a cross section of the human pelvis.

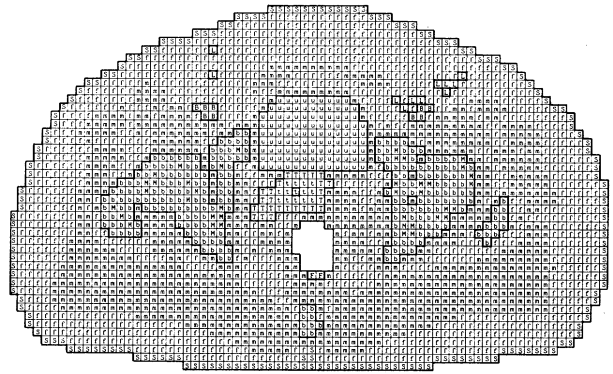


Fig. 3. Subdivision into squares of size 0.005 m \times 0.005 m for the model cross section of the human pelvis. The symbols inside the squares refer to the material composition of the tissue (see Table III).

In view of the application to hyperthermia techniques the quantity to be computed is the volume density of generated heat power, averaged over a period of the electromagnetic oscillations. This quantity is [7]

$$\dot{w}_h = \frac{1}{2} \sigma |E|^2. \quad (13)$$

A. Discretization and Numerical Results

Numerical results are presented for the generated heat power in a model of the cross section of the human pelvis (Fig. 2), the latter as constructed from an X-ray computer tomographic scan [6]. This cross section is subdivided into squares of size 0.005 m \times 0.005 m (Fig. 3). The frequency of operation of the electromagnetic irradiation is taken to be 27 MHz. The electromagnetic parameters of tissue used in our computer program are listed in Table III [6]–[15]. In order to reduce the absorption of the electromagnetic radiation in the bladder, the latter is, in this model, assumed to be continuously flushed with distilled water.

The incident field is computed from (3). Experiments have shown that the aperture field is practically constant and falls off rapidly near the edges, where it reduces to zero. Therefore, we have approximated $E^a(\mathbf{x}')$ by a constant value. Since the actual distances between the points of observation and the points of the aperture are small compared to the free-space wavelength, we can replace the Hankel function occurring in the Green's function by the first two terms of its power-series

TABLE III
ELECTROMAGNETIC PARAMETERS (AT 27 MHz) OF TISSUE USED IN THE
COMPUTER PROGRAM

name	ϵ_r	σ (S/m)
blood (B)	118	1.1
bone (b)	7.3	0.028
fat (f)	20	0.047
faeces (F)	113	0.6
lymph node (L)	200	0.65
marrow (M)	200	0.65
muscle (m)	113	0.61
skin (s)	113	0.61
tumor (T,t)	60	0.8
"urine" flush (U)	72.5	0.002
full bladder (u)	50	1.44
air ()	1	0

expansion. The remaining integral over the aperture can then be calculated analytically.

The total field inside the body is computed with the aid of the iteration scheme shown in Table II. The integrals over the domain D occupied by the body are replaced by the summation of the integrals over the square subdomains (cf. Fig. 3). Over each square the field functions $E^{(n)}$, $C^{(n)}$, $F^{(n)}$, $e^{(n)}$, and $f^{(n)}$ (cf. Table II) are assumed to have constant values. For small values of its argument, the Hankel function (in the Green's function) occurring in an integral over a square is replaced by the first two terms of its power-series expansion. The relevant integration can then be carried out analytically. For larger values of its argument, the Hankel function occurring in an integral over a square is simply replaced by its value at the midpoint of the relevant square subdomain and a subroutine for the Hankel function is used. In this way, all integrations in the iteration scheme reduce to simple summations over values at the centers of each of the squares. It is noted that the subdivision of the body into identical squares leads to a substantial reduction in computation time and memory usage, since the integrals over the squares containing the Hankel functions need to be evaluated for the set of actual distances between the centers of the different squares only.

For deep-seated tumors, as is the case in Fig. 2, it seems advantageous to irradiate the body from two sides simultaneously. To avoid the possibly strong interference phenomena (standing-wave patterns) that would occur if the two radiators operate at exactly the same frequency, the radiators are tuned to slightly different frequencies. In this case, the time-averaged generated heat power is the sum of the contributions of the two radiators separately. This procedure, too, has been carried out numerically. The convergence of the iterative procedure appears to be very satisfactory (Table IV). We have stopped the procedure after three iterations. Fig. 4 shows the computer output of the normalized distribution of the volume density of generated heat power, i.e., \dot{w}_h/\dot{W}_h , where

$$\dot{W}_h = \int_D \dot{w}_h(\mathbf{x}) dA(\mathbf{x}) \quad (14)$$

denotes the total generated heat power in a unit height (m) of the body, averaged over a period of the electromagnetic oscil-

TABLE IV
NORMALIZED ROOT-MEAN-SQUARE ERROR AS A FUNCTION OF THE NUMBER
OF ITERATIONS (ONLY THE UPPER RADIATOR OF FIG. 4 IS ACTIVE)

number of iterations	$[\text{ERR}^{(n)}/\text{ERR}^{(0)}]^2$
$n = 0$	100%
$n = 1$	18%
$n = 2$	4%
$n = 3$	3%

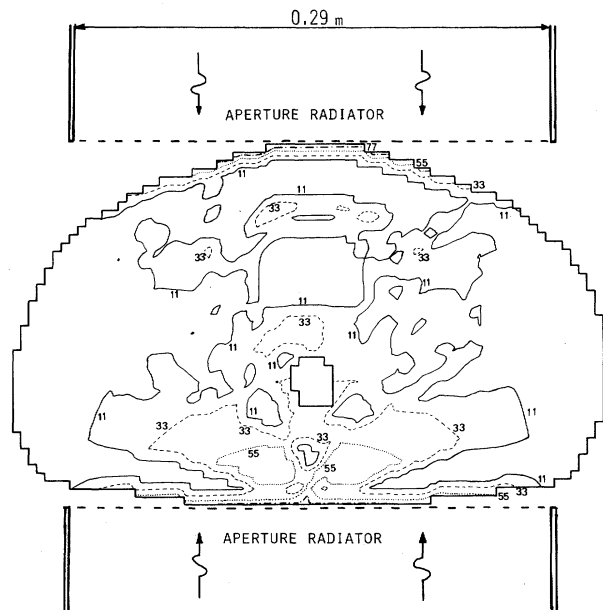


Fig. 4. Computed lines of equal distribution of the volume density of generated heat power in the tissue model of the cross section of the human pelvis;

- $\dot{w}_h/\dot{W}_h = 11 \text{ m}^{-2}$
- - - $\dot{w}_h/\dot{W}_h = 33 \text{ m}^{-2}$
- $\dot{w}_h/\dot{W}_h = 55 \text{ m}^{-2}$
- $\dot{w}_h/\dot{W}_h = 77 \text{ m}^{-2}$

lations. Since the next step involves the computation of the temperature distribution taking full account of the diffusion of heat, the quantity \dot{w}_h is the input parameter for this computation rather than the specific absorption rate SAR recommended in [7].

From the results it follows that the heat generation is higher in the tumor than in the surrounding tissue, which consists mainly of fat. Further, very high values of heat generation occur in the neighborhood of the radiating apertures. Any unwanted effects of the latter can be negated by superficial cooling of the skin.

The computed distribution of \dot{w}_h serves as the input to the computer program that yields the temperature distribution in the tissue as a function of time. This will be discussed in Section III.

III. THE HEAT TRANSFER PROBLEM

In this section we investigate the heat transfer part of the problem, i.e., the computation of the temperature distribution in the tissue as it results from the heat electromagnetically generated in it. The physical quantities and the constitutive parameters that play a role in the computation of the tempera-

TABLE V
PHYSICAL QUANTITIES AND CONSTITUTIVE PARAMETERS OCCURRING IN
THE HEAT-CONDUCTION PROBLEM

name	symbol	SI-unit
time	t	s
temperature	T	K ($^{\circ}\text{C}$)
volume density of generated heat power	\dot{w}_h	W/m ³
volume density of extracted heat power	\dot{w}_c	W/m ³
thermal conductivity	κ	W/m $^{\circ}\text{C}$
volume density of mass	ρ	kg/m ³
specific heat capacity	c	J/kg $^{\circ}\text{C}$
blood flow rate	F	m ³ /kg s

ture distribution in inhomogeneous tissues are listed in Table V. Although the SI unit of the temperature is prescribed as K, for practical reasons, we have taken $^{\circ}\text{C}$ as the unit for the temperature.

The temperature distribution is governed by [19]

$$\rho c \partial_t T - \text{div}(\kappa \text{grad } T) = \dot{w}_h - \dot{w}_c(\mathbf{x}, T) \quad (15)$$

where, in the range of temperatures where hyperthermia is applied, the change of \dot{w}_h , ρ , κ , and c with temperature can be ignored. The function \dot{w}_h represents the joule heat dissipation by the electromagnetic irradiation, while \dot{w}_c represents the heat extraction due to blood circulation. This partial differential equation must be supplemented by the initial conditions and the boundary conditions. Let $t = 0$ be the instant at which the source of heat generation is switched on, then we have

$$\lim_{t \rightarrow 0} T = T_0 \quad (16)$$

where T_0 is the equilibrium temperature of the body (usually $T_0 = 37^{\circ}\text{C}$). As boundary conditions we have either

$$T = \text{constant (isothermal surface)} \quad (17)$$

or

$$\partial_n T = 0 (\text{heat-insulating surface}) \quad (18)$$

where ∂_n is the derivative in the direction of the normal to the surface. In the present analysis we use the x_3 -independent two-dimensional form of (15).

A. Discretization and Numerical Results

Numerical results are presented for the temperature distribution in the tissue model shown in Fig. 3, while the applied source strength of heat generation is shown in Fig. 4. The parameters pertaining to the heat-conduction in the tissue as used in our computer program are listed in Table VI [6]–[9], [16]. The temperature of the distilled water flush through the bladder is held at 42°C ; this high temperature is chosen because of the positive influence it has on the hyperthermic therapy. Further, the cooling function \dot{w}_c due to the blood flow is chosen to be [7]–[9]

$$\dot{w}_c = (F\rho)_{\text{tissue}} \times (\rho c)_{\text{blood}} \times (T - 37) \quad (19)$$

in which F denotes the rate of the blood flow through the tissue. Due to the effect of vasodilation at elevated temperatures, the quantity F is temperature dependent. Although this

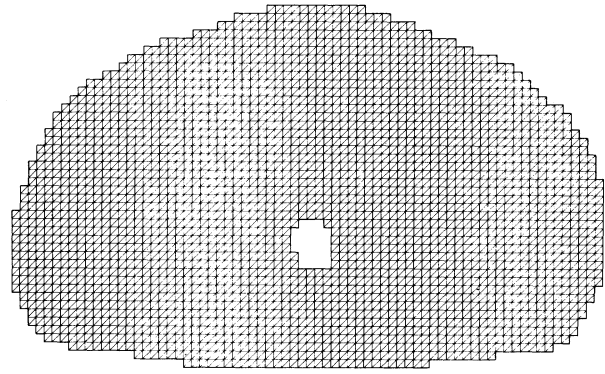


Fig. 5. Mesh generated by the finite-element procedure.

dependence can be taken into account in the applied numerical scheme, in the present analysis we have taken F to be its basal value (cf. Table VI). For a more refined analysis, more accurate data for F as a function of temperature are needed [6]. For the same reason the blood temperature is kept at 37°C . The cooling due to the blood flow through the tumor is chosen to decrease from the periphery (T) to its center (t). In the most deep-seated element of the tumor (Fig. 3), blood circulation is assumed to be very low and, therefore, the cooling is neglected. In the feces region the cooling is set equal to zero and the raise in temperature is computed. Finally, we have assumed that the body is cooled superficially from outside and held at the temperature $T = 30^{\circ}\text{C}$.

The partial differential equation (15) with initial condition (16) has been solved numerically using a finite-element technique [20] in space and a finite-difference method in time, the so-called method of lines [21]. For the discretization of the spatial part the standard Galerkin method with linear finite elements (for the mesh see Fig. 5) has been used [22]. The resulting system of ordinary differential equations in time is then solved using Euler's explicit method [23]. In accordance with the discretization of the electromagnetic problem, the squares of $0.005 \text{ m} \times 0.005 \text{ m}$ are each subdivided in two triangular domains, the number of cells now amounting to 5000 (Fig. 5). This number is dictated by the high gradients of the temperatures in some regions.

In Figs. 6–8, we show the computed temperature distribution in the tissue after $t = 360, 720$, and 1440 s of electromagnetic irradiation, with the total amount of generated heat power in the body per unit length of the axial direction chosen as $\dot{W}_h = 1600, 2300$, and 3600 W/m . Fig. 6 shows that, for $\dot{W}_h = 1600 \text{ W/m}$, a partial heating of the tumor is obtained up to local temperatures of approximately 45°C . After about twenty-four minutes a steady state is reached and the high temperature only occurs in the tumor. For $\dot{W}_h = 2300 \text{ W/m}$, Fig. 7 shows that an essential larger part of the tumor is overheated, i.e., it reaches a temperature higher than 42°C , while all other parts of the body have temperatures lower than 42°C . Finally, Fig. 8 shows that, for $\dot{W}_h = 3600 \text{ W/m}$, the total generated heat-power is too high: not only the tumor but also other parts of our model of the body are overheated.

Note that in all cases high temperatures occur in the feces region.

We have also made a computer run where the bladder is assumed to be full (for the parameters employed see Tables III

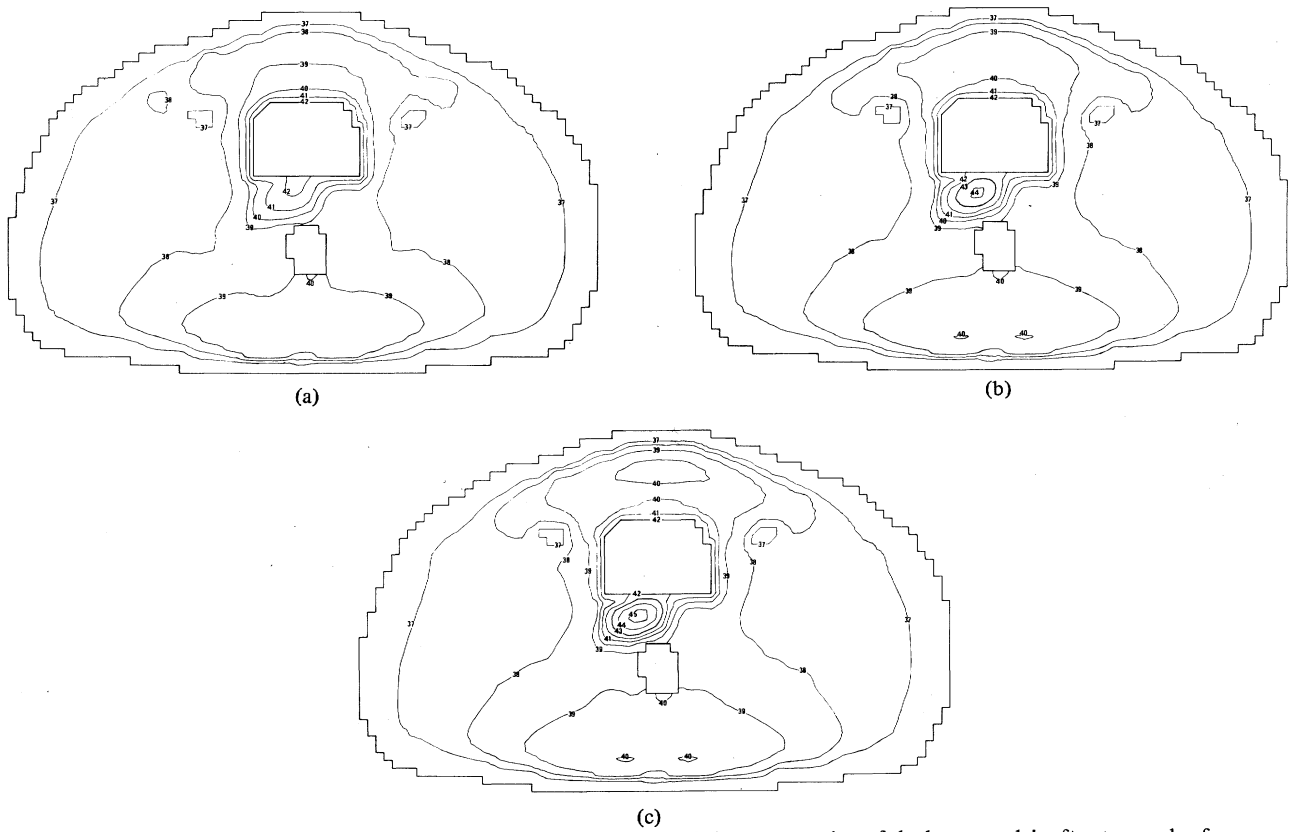


Fig. 6. Computed temperature distribution in the tissue model of the cross section of the human pelvis after t seconds of electromagnetic irradiation ($\dot{W}_h = 1600$ W per length in the axial direction); (a) $t = 360$ s, (b) $t = 720$ s, (c) $t = 1440$ s.

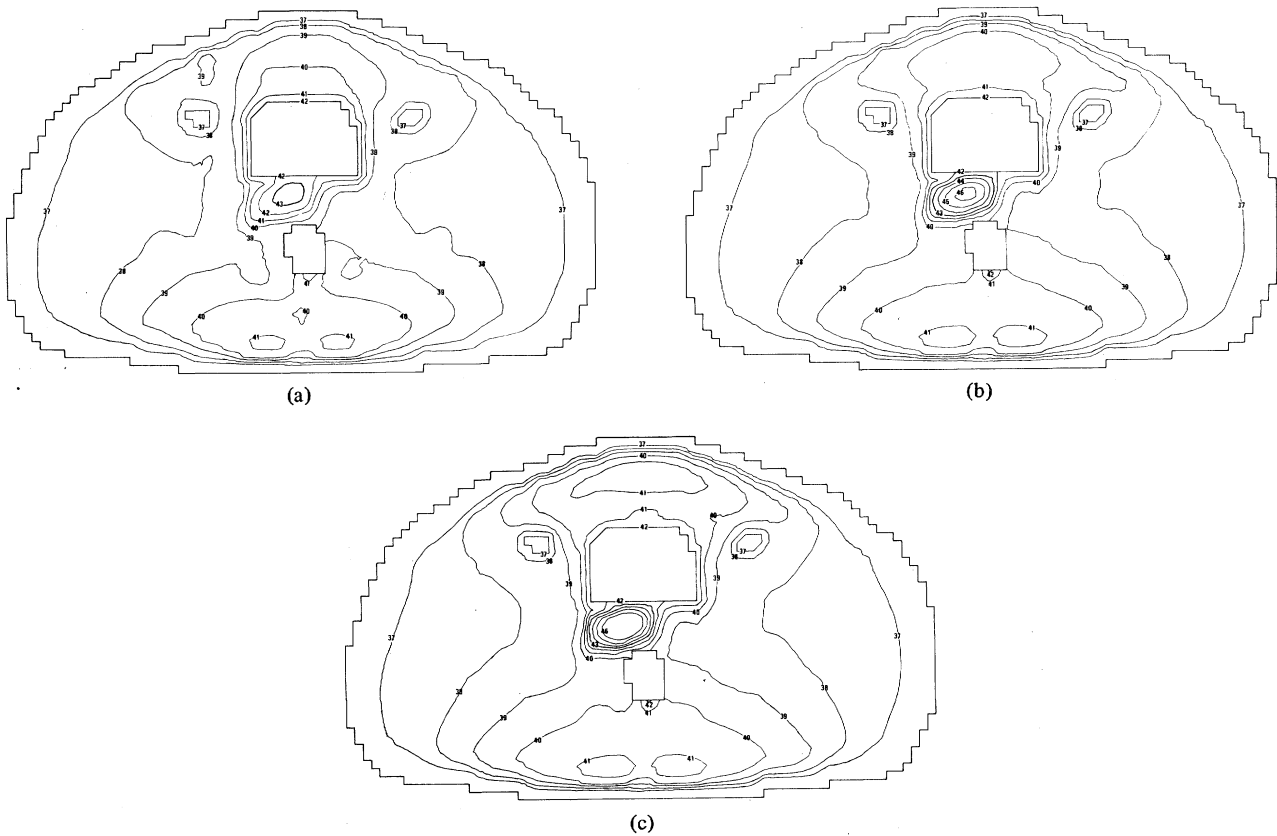


Fig. 7. Computed temperature distribution in the tissue model of the cross section of the human pelvis after t seconds of electromagnetic irradiation ($\dot{W}_h = 2300$ W per length in the axial direction); (a) $t = 360$ s, (b) $t = 720$ s, (c) $t = 1440$ s.

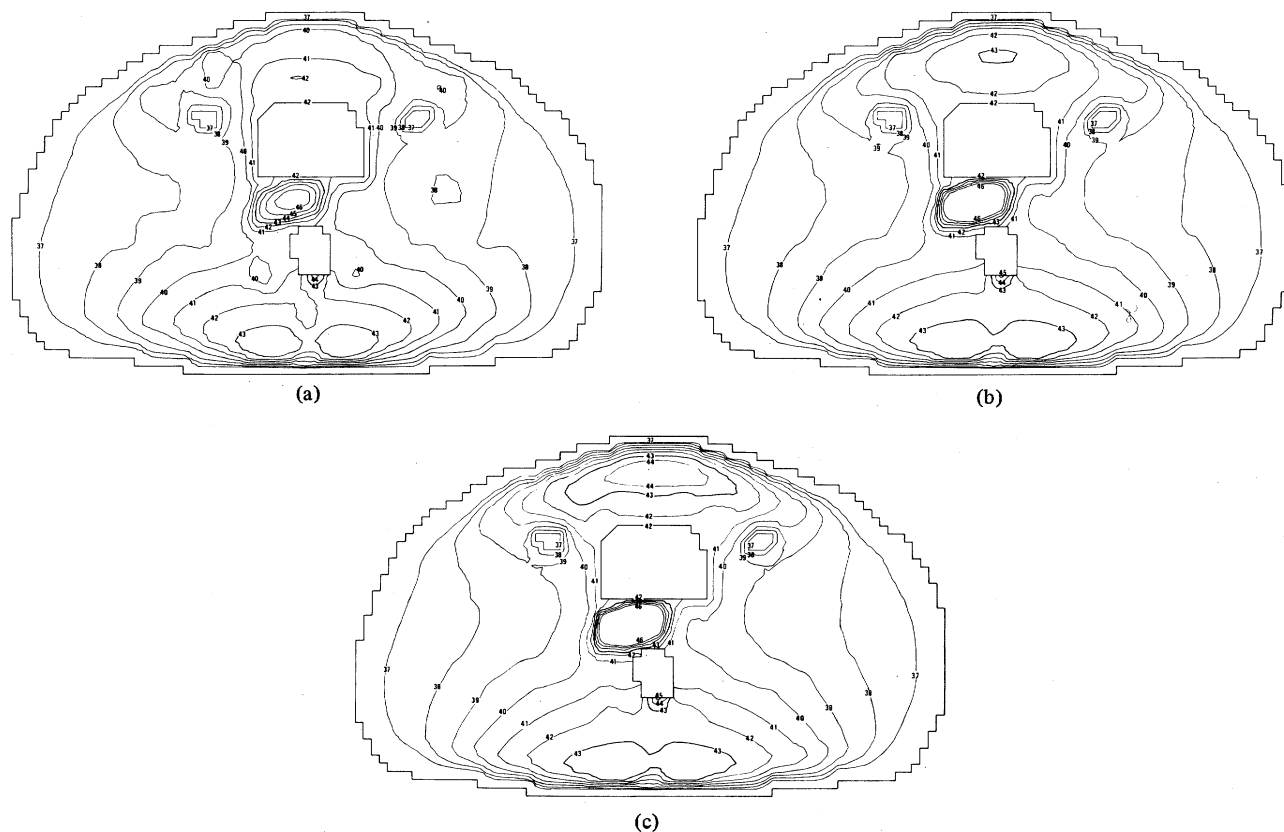


Fig. 8. Computed temperature distribution in the tissue model of the cross section of the human pelvis after t seconds of electromagnetic irradiation ($\dot{W}_h = 3600$ W per length in the axial direction); (a) $t = 360$ s, (b) $t = 720$ s, (c) $t = 1440$ s.

TABLE VI
HEAT-CONDUCTION PARAMETERS OF TISSUE USED IN THE COMPUTER PROGRAM

name	κ (W/m °C)	ρ (kg/m ³)	c (J/kg °C)	F (m ³ /kg s)	boundary condition
blood (B)		1.06×10^3	3.96×10^3		$T = 37^\circ\text{C}$
bone (b)	0.436	1.79×10^3	1.3×10^3	4.2×10^{-7}	
fat (f)	0.22	0.9×10^3	2.3×10^3	5×10^{-7}	
faeces (F)	0.6	1×10^3	3.9×10^3	0	
lymph node (L)	0.515	1.1×10^3	3.96×10^3	7.5×10^{-6}	
marrow (M)	0.515	1.1×10^3	3.96×10^3	7.5×10^{-6}	
muscle (m)	0.6	1.02×10^3	3.5×10^3	8.3×10^{-6}	
skin (S)	0.498	1×10^3	3.5×10^3	1.67×10^{-5}	
tumor periphery (T)	0.57	1.04×10^3	3.9×10^3	1.67×10^{-6}	
tumor center (t)	0.57	1.04×10^3	3.9×10^3	5×10^{-7}	
"urine" flush (U)					$T = 42^\circ\text{C}$
full bladder (U)	0.561	1.02×10^3	3.9×10^3	0	
air ()					$a_n T = 0$
body surface					$T = 30^\circ\text{C}$

and VI). It turned out that after 360 s already the temperature in the bladder was 50°C [for comparison to a flushed bladder see Fig. 7(a)], while under influence of thermal diffusion the entire neighborhood of the bladder also reaches a prohibitively high temperature. Therefore, flushing of the bladder is an absolute necessity.

Another effect we investigated was the influence of the blood

flow in the tumor tissue. As compared to the results of Fig. 7, the corresponding ones where $F = 1.67 \times 10^{-6} \text{ m}^3/\text{kg} \cdot \text{s}$ through the entire tumor showed a temperature distribution that negligibly deviated from Fig. 7.

As far as the rate of blood flow in the cooling tissues (muscles) is concerned, this must remain at a high enough value for the tumor to be sufficiently heated. In this respect we have made a computer run where the value of F was taken to be one third of the actual value in muscular tissue; the result was that the temperature in the muscle became higher than in the tumor.

IV. CONCLUSIONS

From our analysis it may be inferred that the temperature can indeed be higher in the tumor than elsewhere in the body. It is likely from this model that pelvic tumors can be heated efficiently. It should be noted, however, that while the chosen values of the physical parameters of tissue are realistic, they may eventually require correction when more human data become available. For example, some of the values are the measured values of pig tissue, the latter probably behaving differently from human tissue. Also, the estimates of the blood flow values in the various tissues, including tumor, may require adjustment. A more detailed analysis of the values of the physical parameters of tissue, together with suitable references to the existing literature, is expected to become available in the near future [6].

V. COMPUTATIONAL ASPECTS

All computations have been performed on the Amdahl 470/V7B computer of the Computing Centre of the Delft University of Technology.

The program with respect to the electromagnetic part has been written in the PL1-language (a Fortran version is available, too). The computation time needed by our program to obtain the numerical results of the distribution of generated heat power in the body amounts to about 900 s. This computation time is largely determined by the size of the mesh representing the discretized distribution of tissue. This mesh size must be sufficiently small to cover the phase and amplitude changes of the field (the latter is for the polarization under consideration, continuous through a discontinuity in tissue) and the changes in physical parameters. Now, at the assumed frequency of operation of 27 MHz (wavelength in the tissue in the order of 1 m), the computation time can be substantially reduced by taking, for the computation of the field distribution, a much wider mesh than is necessary to cover the changes in physical parameters. In the first instance, the values of the physical parameters ϵ_r and σ over these larger squares are then taken to be the averages of the values of ϵ_r and σ over the relevant sub-squares. Next, the generated heat power $\frac{1}{2} \sigma |E|^2$ is computed in the centers of the squares of the finer subdivision (Fig. 3) necessary to recover the original values of \dot{w}_h . For the used frequency of operation of 27 MHz, this averaging procedure using squares of $0.02 \text{ m} \times 0.02 \text{ m}$ does not change the final numerical results of the generated heat power, at least not within the 3 percent accuracy that we have imposed. In this way, the computation time needed can be reduced from about 900 s to about 15 s.

The problem with respect to the heat-conduction part of the problem has been written in the Fortran language. The time needed to compute the temperature evolution in the body (as shown in, e.g., Fig. 6) amounts to about 40 s. Since the differential equation at hand is "stiff" (the size of the time step has an upper bound for stability reasons rather than for accuracy requirements), some reduction in computation time might be obtained by increasing the time step and using a more sophisticated method [24] for the integration in time. A study as to this time integration is under progress.

Having reduced, on the powerful Amdahl 470/V7B computer, the computation time and storage requirements to the lower values, we have run a Fortran version of the entire program on the much smaller PDP-11/70 computer. On the latter, the computation time was 20 min for the electromagnetic problem and 20 min for the heat conduction problem.

ACKNOWLEDGMENT

The authors wish to acknowledge the stimulating support of the Department of Experimental Radiotherapy (Prof. H. S. Reinhold, G. C. van Rhooen, J. L. Wike-Hooley), Erasmus University, Rotterdam, The Netherlands. This includes the discussions as regards hyperthermic cancer therapy, the composition of the cross section of the human pelvis constructed from an X-ray computer tomographic scan and the values of the relevant physical parameters of tissue. Further, we would like to

thank Prof. T. Poorter (Delft University of Technology, Department of Electrical Engineering, Delft, The Netherlands) and Dr. J. J. Batterman (Antoni van Leeuwenhoek hospital, City University of Amsterdam, Laboratory of Radiology, The Netherlands) for their stimulating pressure to start the research presented in this paper.

REFERENCES

- [1] J. Gordon Short and P. F. Turner, "Physical hyperthermia and cancer therapy," *Proc. IEEE*, vol. 68, pp. 133-142, 1980.
- [2] M. F. Iskander, R. Maini, C. H. Durney, and D. G. Bragg, "A microwave method for measuring changes in lung water content: Numerical simulation," *IEEE Trans. Biomed. Eng.*, vol. BME-25, pp. 797-803, 1981.
- [3] M. F. Iskander and C. H. Durney, "Medical diagnosis and imaging using electromagnetic techniques," in *Theoretical methods for determining the interaction of Electromagnetic Waves With Structures*, J. K. Skwirzynski, Ed. NATO Advan. Study Inst. Series, Series E: Appl. Sci. no. 40, Sijthoff and Noordhoff, Alphen aan de Rijn, The Netherlands, 1981, pp. 835-854.
- [4] M. F. Iskander, P. F. Turner, J. B. Dubow, and J. Kao, "Two-dimensional technique to calculate the EM power deposition pattern in the human body," *J. Microwave Power*, vol. 17, pp. 175-185, 1982.
- [5] G. C. Herman and P. M. van den Berg, "A least-square iterative technique for solving time-domain scattering problems," *J. Acoust. Soc. Amer.*, vol. 72, pp. 1947-1953, 1982.
- [6] The cross-section model of the human pelvis and the estimated values of the relevant physical parameters of tissue were furnished by the Department of Experimental Radiotherapy (Prof. H. S. Reinhold, G. C. van Rhooen, J. L. Wike-Hooley), Erasmus University, Rotterdam, The Netherlands. A more detailed study as to the accuracy of the published values of the relevant physical and physiological parameters is being continued.
- [7] NRCP Rep. No. 67, "Radiofrequency electromagnetic fields, properties, quantities and units, biophysical interaction, and measurements," Nat. Coun. Radiation Protection and Measurements, Washington, DC, 134 pp., 1981.
- [8] R. K. Jain and P. M. Gullino, Eds., "Thermal characteristics of tumors: Application in detection and treatment," *Ann. N.Y. Acad. Sci.*, vol. 335, 542 pp., 1980.
- [9] A. W. Guy, "History and state of art on the quantitation of the interaction of electromagnetic fields with biological structures," in *Theoretical Methods for Determining the Interaction of Electromagnetic Waves with Structures*, J. K. Skwirzynski, Ed. NATO Advan. Study Inst. Series, Series E, Appl. Sci. no. 40, Sijthoff and Noordhoff, Alphen aan de Rijn, The Netherlands, 1981, pp. 781-816.
- [10] H. F. Schwan and G. M. Piersal, "The absorption of electromagnetic energy in body tissues, Part 1," *Amer. J. Phys. Med.*, vol. 33, pp. 371-404, 1954.
- [11] —, "The absorption of electromagnetic energy in body tissues, Part II," *Amer. J. Phys. Med.*, vol. 34, pp. 425-448, 1955.
- [12] H. Cook, "The dielectric behavior of some types of human tissues at microwave frequencies," *Brit. J. Appl. Phys.*, vol. 2, p. 295, 1951.
- [13] —, "Dielectric behavior of human blood at microwave frequencies," *Nature*, vol. 168, p. 247, 1951.
- [14] —, "A comparison of the dielectric behavior of pure water and human blood at microwave frequencies," *Brit. J. Appl. Phys.*, vol. 3, p. 249, 1952.
- [15] K. Cole and R. Cole, "Dispersion and absorption in dielectrics," *J. Chem. Phys.*, vol. 9, p. 34, 1941.
- [16] A. W. Guy, J. F. Lehmann, and J. B. Stonebridge, "Therapeutic applications of electromagnetic power," *Proc. IEEE*, vol. 62, pp. 55-75, 1974.
- [17] D. S. Jones, *The Theory of Electromagnetism*. Elmsford, NY: Pergamon, 1964, 807 pp.
- [18] J. H. Richmond, "Scattering by a dielectric cylinder of arbitrary cross-section shape," *IEEE Trans. Antennas Propagat.*, vol. AP-13, pp. 334-341, 1965.
- [19] M. M. Chen and P. Pantazatos, "Tomographical thermography," in *Thermal Characteristics of Tumors: Application in Detection*

and Treatment, R. K. Jain and P. M. Gullino, Eds. *Ann. N.Y. Acad. Sci.*, vol. 335, 542 pp., 1980.

- [20] A. Segal, *AFEP User Manual*, Delft University of Technology, Delft, The Netherlands, 1981.
- [21] A. R. Mitchell and D. F. Griffiths, *The Finite Difference Method in Partial Differential Equations*, London, England: Wiley, 1980, 272 pp.
- [22] G. Strang and G. J. Fix, *An Analysis of the Finite Element Method*. Englewood Cliffs, NJ: Prentice Hall, 1973, 306 pp.
- [23] J. D. Lambert, *Computational Methods in Ordinary Differential Equations*. London, England: Wiley, 1971, 278 pp.
- [24] A. Segal and N. Praagman, "The finite element method for time-dependent problems," *Delft Prog. Rep.*, vol. 2, pp. 119-130, 1977.



Peter M. van den Berg was born in Rotterdam, The Netherlands, on November 11, 1943. He received the degree in electrical engineering from the Polytechnic School of Rotterdam, Rotterdam, The Netherlands, in 1964, the B.Sc. and M.Sc. degrees in electrical engineering in 1966 and 1968, respectively, and the Ph.D. degree in technical sciences in 1971, all from the Delft University of Technology, Delft, The Netherlands.

From 1967 to 1968 he was employed as a Research Engineer by the Dutch Patent Office. From 1968 to the present he has been a member of the Scientific Staff of the Electromagnetic Research Group of the Delft University of Technology. During these years he carried out research and taught classes in the area of wave propagation and scattering problems. During the academic year 1973-1974 he was a Visiting Lecturer in the Department of Mathematics, University of Dundee, Scotland. During a three-month period of 1980-1981, he was a Visiting Scientist at the Institute of Theoretical Physics, Goteborg, Sweden. He was appointed Professor at the Delft University of Technology in 1981.



A. T. De Hoop was born in 1927 in Rotterdam, The Netherlands. He received the M.Sc. degree in electrical engineering and the Ph.D. degree from the Delft University of Technology, Delft, The Netherlands, in 1950 and 1958, respectively. In 1982 he received the Honorary Doctor's degree in applied sciences from the State University of Ghent, Belgium.

In 1956-1957 he spent a year at the Institute of Geophysics, University of California at Los Angeles, where he performed research on elas-

todynamic diffraction theory. Since 1960 he has been a Professor of Electromagnetic Theory and Applied Mathematics at the Delft University of Technology. His research concentrates on analytical and numerical techniques in electromagnetic, acoustic, and elastodynamic wave diffraction. He spent a sabbatical leave in 1976-1977 at Philips Research Laboratories, Eindhoven, The Netherlands, where he performed research on field problems in magnetic-recording configurations. In 1982 he was a Summer's Visiting Scientist at Schlumberger-Doll Research, Ridgefield, CT.

Dr. De Hoop is a member of the Royal Institution of Engineers in The Netherlands, The Netherlands Institute of Electronic and Radio Engineers, and the Dutch Mathematical Society.



A. Segal was born in The Hague, The Netherlands, in 1948. He received the M.Sc. degree in mathematical engineering from the Delft University of Technology, Delft, The Netherlands, in 1971.

Currently he is a staff member of the Numerical Analysis Group of the Delft University of Technology.



N. Praagman was born in Drachten, The Netherlands, in 1947. He received the M.Sc. degree in applied mathematics from the Free University of Amsterdam, The Netherlands, in 1971, and the Ph.D. degree in technical sciences from the Delft University of Technology, Delft, The Netherlands, in 1979.

Currently he is affiliated with Svasek B.V., Coastel and Harbour Engineering Consultants, The Netherlands, and with the Dutch National Institute of Water Supply, The Netherlands.